doi:10.3788/gzxb20164507.0710004

# 基于单相机-双棱镜的小型三维指纹获取系统

卢宝莉,刘育梁,王新伟
(中国科学院半导体研究所 光电系统实验室,北京 100083)

**摘 要**:提出了一种小型非接触式三维指纹获取系统.该系统采用单个 CCD 相机作为图像传感器,利用相机镜头结合双棱镜的成像装置在单帧 CCD 图像上获得立体图像对,再基于立体视觉原理重建三维指纹.整个系统封装后尺寸为 12 mm×12 mm×10 mm.基于该系统进行了指纹获取实验,测量的均方根误差为 0.022 mm.该系统操作简单且结构紧凑,为三维指纹的获取提供了一种小型化方案.

**关键词**:指纹识别;获取系统;双目立体视觉;成像装置;小型化
**中图分类号**:O439 **文献标识码**:A **文章编号**:1004-4213(2016)07-0710004-6

# Compact Three-dimensional Fingerprint Acquisition System Based on a Single Camera with a Biprism

LU Bao-li, LIU Yu-liang, WANG Xin-wei
(*Optoelectronic System Laboratory, Institute of Semiconductors, Chinese Academy of Sciences, Beijing* 100083, *China*)

**Abstract**: A compact touchless 3D fingerprint acquisition system was proposed in this paper. The system utilizes a single CCD camera as an image sensor and combines the CCD with a biprism to obtain stereo image pairs in one frame of the CCD. Then 3D fingerprint is established based on the stereo vision technique. The entire size of the compact encapsulated system is 12 mm × 12 mm × 10 mm. The experiment of a forefinger fingerprint acquisition was conducted based on this system and the measurement root mean square error is 0.022 mm. This work is expected to provide a miniaturized solution for 3D fingerprint acquisition with its easy operation and compact structure.

**Key words**: Fingerprint identification; Acquisition system; Binocular stereo vision; Imaging device; Miniaturization
**OCIS Codes**: 100.3010; 330.1400; 330.5000; 150.0150;120.4820

## 0 Introduction

Human recognition based on biometrics is widely applied in many fields like government, army, bank, e-commerce, security defense, social welfare safeguard, and so on. Some biometric features such as iris, face, fingerprint, voice, hand geometry, and the retinal pattern of eyes have been used to confirm the identity of a certain person[1-2]. Among all these features, the fingerprint is considered as the most popular and reliable technique for an automatic personal identification[3].

Conventional fingerprint systems usually require the placing and pressing of fingers against a hard surface, such as glass or silicon. Because the skin of the finger is not flat, the user must apply enough pressure on the surface to obtain a sufficient size of the fingerprint and achieve a good image quality.

**Foundation item**: The National Natural Science Foundation of China (Nos. 61205019, 61475150)
**First author**: LU Bao-li(1990—), female, Ph. D. degree candidate, mainly focuses on binocular stereo vision technique. Email:lubaoli@semi.ac.cn
**Supervisor**: LIU Yu-liang(1966—), male, professor, Ph. D. degree, mainly focuses on intelligent scientific instruments and optical fiber communication. Email:ylliu@semi.ac.cn
**Received**: Dec. 11, 2015; **Accepted**: Jan. 26, 2016

However, an unavoidable physical distortion in arbitrary directions is produced by this pressure. It may make each fingerprint image from the same finger appear quite different. In addition, the improper finger placement, slippage, smearing of finger and reside of finger dirt often result in partial or degraded quality images[4]. Besides, the touching fingerprint collection method may also cause the propagation of diseases from a hygiene point of view. To overcome these disadvantages, a touchless three-dimensional (3D) fingerprint recognition technique is introduced recently[5-8]. It can provide hygienic solutions to such problems and can cope up with the residue of previous fingerprint impressions which can also be a potential security threat[9].

One of the most important aspects in the touchless 3D fingerprint recognition is the 3D fingerprint acquisition, which is an essential problem of the 3D surface reconstruction[10]. Up to now, there are three mainly 3D reconstruction techniques for 3D fingerprint of laser scanning[11-13], structured light imaging[14-16], and multi-view reconstruction[17-19]. In Ref. [16], a structured light system which contains a synchronized camera and a projection device is proposed for the 3D fingerprint reconstruction. The authors can achieve a 3D model of the fingerprint in less than one second by projecting a sequence of strip patterns onto the finger surface and imaged by the camera. In Ref. [17], 3D fingerprints are reconstructed based on three views of fingerprint images. It has been proved that these systems are effective for 3D fingerprint reconstruction. However, these existing systems usually have large volumes and complex structures because of the essence of imaging technologies employed in them. For example, the system in Ref. [16] requires a high speed camera and a specialized projector to implement the 3D fingerprint scanning while the experimental system in Ref. [17] consists of three cameras and four blue Light Eemitting Diodes (LED) lights. The drawback results in lack of popularity of such touchless 3D fingerprint systems. Therefore, the development of more simple and portable 3D fingerprint reconstruction systems is necessary.

In this paper, a compact 3D fingerprint acquisition system that based on binocular stereo vision technique is proposed. It is different from the traditional approach which the images from different views are captured by two or more cameras simultaneously or by changing camera positions with multiple acquisitions[17-18], the system only uses one camera and can reconstruct 3D fingerprint within a single frame.

## 1 3D fingerprint acquisition system

The schematic diagram of the imaging device of the proposed system is shown in Fig. 1 (a). A color Charge-Coupled Diode (CCD) camera with 480 × 640 pixels is employed. An annular array of LEDs is used to provide uniform illumination. In addition, a biprism is fixed before the camera lens, aligning the centerline of the biprism with the centerline of the CCD. The entire acquisition system (not including the image display module) is encapsulated in a small box with the size of 12 mm×12 mm×10 mm as shown in Fig. 1(b).

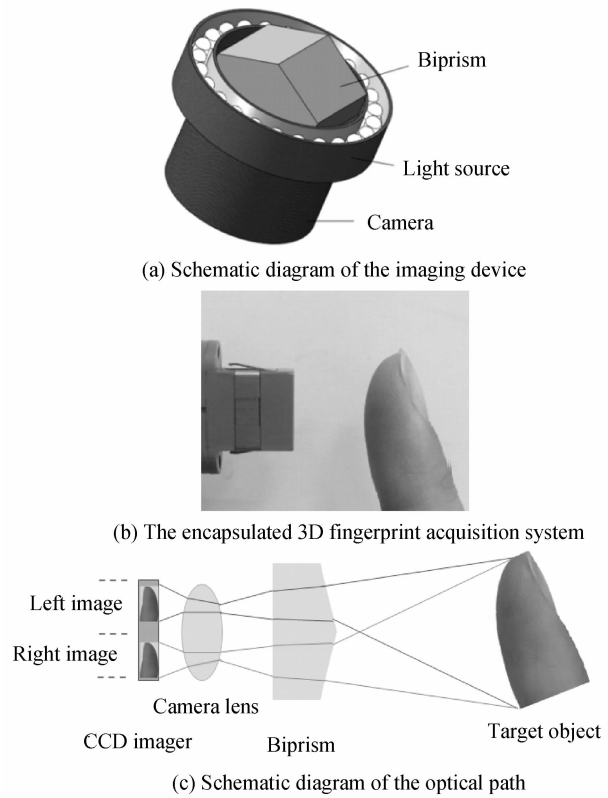


(a) Schematic diagram of the imaging device

(b) The encapsulated 3D fingerprint acquisition system

(c) Schematic diagram of the optical path

Fig. 1 The 3D Fingerprint Acquisition System

Fig. 1 (c) shows the schematic diagram of the optical path. The biprism is employed for forming two perspectives, and thus a two-image pair of a finger can be obtained in a single frame of the CCD from different views. With the biprism, the system is equivalent to have two cameras which are separated by a horizontal distance of the baseline. It is equivalent that the left image comes from the first camera and the right image comes from the second camera. Therefore, a binocular stereo system is built. Then based on the theory of binocular stereo vision, the 3D fingerprint can be reconstructed.

It is worth mentioning that the baseline will be different along with the change of the distance between the biprism and the CCD imager . According to the

relationship among the structural parameters and the resolution of the measurement in the $z$ direction as shown in Eq. (1), the measurement accuracy will increase along with the baseline.

$$\Delta Z=\frac{Z^2 a}{FB+Za} \tag{1}$$

where $\Delta Z$, $a$, $Z$, $F$, $B$ represents the resolution of the measurement in the $z$ direction, the size of CCD pixel, the object distance, focal length and baseline respectively, $a=0.003$ mm.

$F$ is about 2 mm. If the object distance is fixed, according to Eq. (1), a bigger baseline is most definitely better in theory. But taking into account the system size, we adjust the distance between the biprism and the CCD imager to make the baseline about 1.2 mm.

The reconstruction process consists of the following steps: image acquisition, camera calibration, image preprocessing, stereo matching, and 3D view reconstruction. The flow chart explaining the systematic procedure employed in the reconstruction of the 3D fingerprint is shown in Fig. 2. Detail steps of implementing this method will be introduced later.

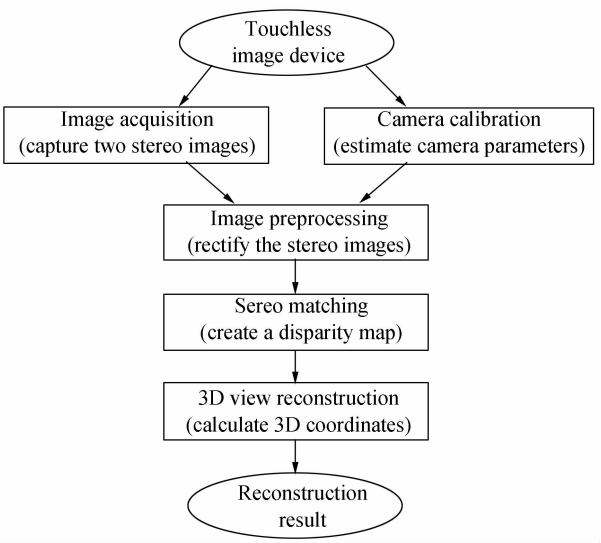


Fig. 2 Flow chart of the proposed acquisition system

## 2 Experimental approach and results

### 2.1 Image acquisition

In the beginning of the reconstruction, a pair of stereo fingerprint images needs to be provided. The expected distance between the camera and the finger is set to 10 mm due to the consideration of image quality. Fig. 3 shows the original image of a forefinger captured by the proposed single stereo camera used in this paper. The image is divided into two parts equally and the image size of each part is restricted to $480\times320$ pixels, as shown in Fig. 4 (a) and (b). Then the left part and the right part of the original image become a pair of stereo images.

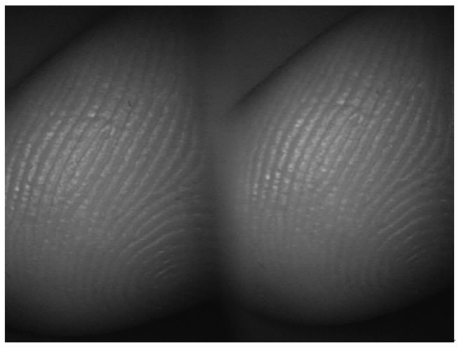

Fig. 3 Original image of a forefinger

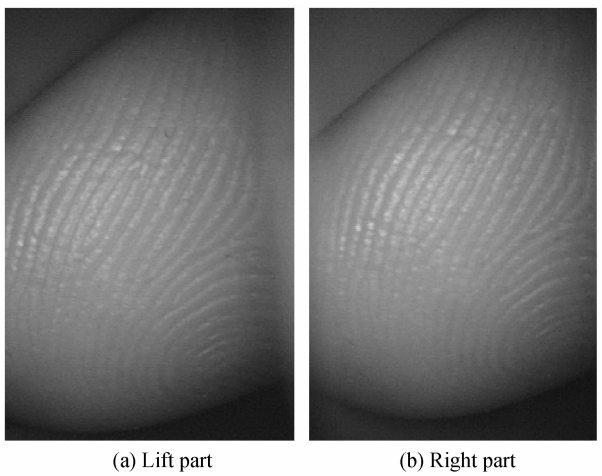


Fig. 4 Two equal parts of the original image

### 2.2 Camera calibration

Camera should be calibrated in the second step, in order to provide camera parameters which can be used to rectify a stereo pair of images and are necessary for 3D reconstruction.

In the experiment, a chessboard pattern is used in the calibration. The size of each square block of the chessboard is 1 mm $\times$ 1 mm. 19 images of the chessboard from different orientations are captured by the single stereo camera. As previously mentioned (in Sec. 2), the system is equivalent to have two cameras with the help of the biprism. It is equivalent that the left part of each image comes from the first camera and the right part comes from the second camera. Thus, we divide every image into two parts equally, and use all the left parts to estimate the intrinsic parameters (*e. g.* focal length, principal point, skew coefficient and distortion) of the first equivalent camera. Then use all the right parts to calibrate the second equivalent camera in the same way. At last, we estimate the translation and rotation of the second equivalent camera relative to the first one. To perform the calibration, the Bouguet camera calibration toolbox[20] is employed. It is based on the method proposed in Ref. [21].

According to the obtained extrinsic parameters (position of the second equivalent camera with respect

to the first equivalent camera), rotation vector $\boldsymbol{R}=[-0.01137\ -0.37638\ -0.00810]$, translation vector $\boldsymbol{T}=[-1.09614\ -0.00663\ -0.32264]$, the spatial configuration of the two cameras and the calibration planes can be calculated. The computing result demonstrates that the built binocular stereo system is actually consistent with the theoretical model. And thus our reconstruction system is proven to be feasible.

### 2.3 Image preprocessing

Epipolar geometry is the most popular theory in the binocular stereo vision domain. However, the built equivalent binocular stereo system does not fulfill the epipolar constraints because of the small angle between the two camera optical axis, some rotations about other axes and the distortion of the lens. In order to employ the ideal binocular stereo model, the pair of stereo images shown in Fig. 4 should be rectified such that parallel and horizontal epipolar lines can be produced in each image. In addition rectification is an important preprocessing step for computing disparity, because it significantly improves the matching speed and accuracy by reducing the 2D stereo correspondence problem to a 1D problem.

The process of image preprocessing is implemented by using the intrinsic and extrinsic parameters obtained previously to transform the images. The preprocessing results are presented in Fig. 5. We can find that the stereo images after rectification are aligned horizontally and there is only a translation in the horizontal direction between the corresponding points. This means that for each point in the left image, its corresponding point in right image lies along the same row.

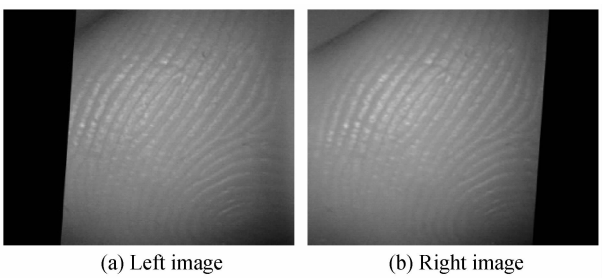


Fig. 5 Stereo images after rectification

### 2.4 Stereo matching

The distance in pixels between corresponding points in the rectified images is called disparity. The disparity is proportional to the distance among the cameras and the 3D world point. Therefore it is used for 3D reconstruction and has a great influence on the reconstruction accuracy. Stereo matching is the process of recognizing the corresponding points between the left image and the right image. To obtain accurate disparity values, a perfect match is very important.

To perform stereo matching and create a dense disparity map, the Semi-Global Block Matching (SGBM) method is employed. It's a variation of the stereo processing by semi-global matching and mutual information which is proposed in Ref. 22. The SGBM algorithm matches blocks rather than individual pixels, and additionally forces similar disparity on neighboring blocks. This additional constraint results in a more complete disparity estimate than the basic Block Matching method.

The algorithm is performed in two steps. Firstly, compute a measure of contrast of the image by using the Sobel filter. Then compute the disparity for each pixel by comparing the Sum of Absolute Differences (SAD) of each block of pixels in the left image.

$$C(u,v,D)=\sum_{u\in S}|I_l(u,v)-I_r(u+D,v)| \tag{2}$$

where $C(u,v,D)$ denotes the matching cost. $I_l(u,v)$ is the intensity of a pixel in the left image with the coordinates $(u,v)$. $I_r(u+D,v)$ is the intensity of the suspected correspondence pixel in the right image. For rectified images the two corresponding pixels are parallel, thus the coordinates of the pixel in the right image are $(u+D,v)$ with $D$ as disparity. $S$ denotes the block region for matching.

The disparity image is determined by selecting for each block the disparity $D$ that corresponds to the minimum cost. Fig. 6 shows the disparity map of the fingerprint images which each disparity value corresponds to a pixel in the left image.


Fig. 6 Disparity map

### 2.5 3D view reconstruction

Once camera parameters and disparity map are both obtained, the 3D world coordinates of points corresponding to each pixel from the disparity map can be calculated. Based on the binocular stereo vision model, we can get the calculation formulas as below by using the stereo triangulation method.

$$\begin{cases} X=\dfrac{Bu_l}{aD} \\ Y=\dfrac{Bv_l}{aD} \\ Z=\dfrac{FB}{aD} \end{cases} \tag{3}$$

where $X$, $Y$, $Z$ are the coordinate values of an object point in the world coordinate system. $u_l$, $v_l$ are the pixel coordinates of the projected point in the left image plane. is the size of CCD pixel. $B$ and $F$ denote the baseline and the focal length of the stereo system respectively. $D$ is the disparity value.

The output of this computation is a 3D point cloud. In order to a better visualization for the texture, the color of each 3D point is also recovered. The dense point cloud is displayed in Fig. 7 which shows the reconstructed 3D view of the fingerprint. As shown in this figure, the texture of the fingerprint is reconstructed clearly.

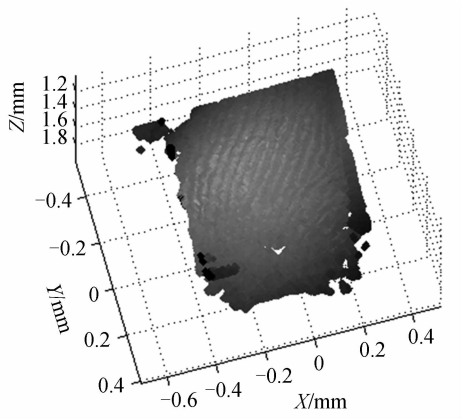


Fig. 7 3D reconstructed view of the fingerprint

## 3 Accuracy analysis of the reconstruction system

In order to analyze the accuracy of the reconstruction system, an experiment is conducted to measure the height of the convex part of a small standard component as shown in Fig. 8. The actual value of the height is 1.98 mm.

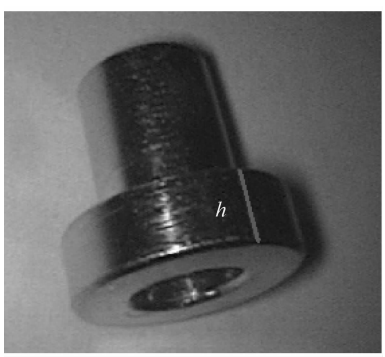


Fig. 8 Small standard component

After calibration, we get that: $B = 1.253$ mm, $F = 2.071$ mm. We reconstruct the component and do the measurement for 10 times. The calculated Root Mean Square Error (RMSE) value is: RMSE = 0.022 mm. The promising experimental result illustrates the good performance of this system. It's able to be comparable to the system whose reconstruction error is within 0.2 mm reported In Ref. [17].

## 4 Conclusion

In fingerprint recognition, the main obstacles for the present 3D fingerprint technologies to replace 2D systems are their complex structure, large volume and high cost. To overcome these drawbacks, a compact touchless 3D fingerprint acquisition system is presented in this paper. The proposed system only uses one camera and can reconstruct 3D fingerprint within a single frame by utilizing a biprism to obtain two different views of fingerprint images. We analyze the rationale of the imaging device firstly. Then we introduce the whole process of the 3D fingerprint reconstruction in details. And the feasibility of the measurement is demonstrated by experiment. The measurement RMSE of the system is 0.022 mm. Furthermore, the entire size of the encapsulated system is 12 mm × 12 mm × 10 mm. It not only reduces the cost but also realizes the miniaturization benefit from the compact structure.

While the surface of the fingerprint has been 3D reconstructed successfully, new problems need to be dealt with, such as the improvement in the reconstruction accuracy and the increase of the reconstruction area. Our future work will focus on developing the stereo matching algorithm which has a better performance on these issues. Moreover, real-time 3D imaging is expected to be explored in the further extension of this work.

**References**

[1] JAIN A K, ROSS A, PRABHAKAR S. An introduction to biometric recognition[J]. *IEEE Transactions on Circuits and Systems for Video Technology*, 2004, **14**(1): 4-20.

[2] LEE C, LEE S, KIM J. A study of touchless fingerprint recognition system[C]. SSPR&SPR 2006: 358-365.

[3] MALTONI D, MAIO D, JAIN A K, *et al*. Handbook of fingerprint recognition[M]. Springer, 2009.

[4] DELAC K, GRGIC M. A survey of biometric recognition methods [C]. Proceedings Elmar-2004: 46th International Symposium Electronics in Marine, T. Kos and M. Grgic, eds. 2004: 184-193.

[5] PARZIALE G, CHEN Y. Advanced technologies for touchless fingerprint recognition[M]. Handbook of Remote Biometrics, London: Springer, 2009: 83-109.

[6] WANG Yong-chang, HASSEBROOK L G, LAU D L. Data acquisition and processing of 3-D fingerprints [J]. *IEEE Transactions on Information Forensics and Security*, 2010, **5**: 750-760.

[7] Tbs, retrieved http://www.tbs-biometrics.com.

[8] KUMAR A, KWONG C. Towards contactless, low-cost and accurate 3D fingerprint identification[C]. IEEE CVPR, 2013: 3438-3443.

[9] HUANG Shu-jun, ZHANG Zong-hua, ZHAO Yan, *et al*. 3D fingerprint imaging system based on full-field fringe projection

profilometry[J]. *Optics and Lasers in Engineering*, 2014, **52**: 123-130.

[10] XIE Wu-yuan, SONG Zhan, ZHANG Xiao-ting, A novel photometric method for real-time 3D reconstruction of fingerprint[C]. IEEE International Symposium on Visual Computing, 2010: 31-40.

[11] GABAI H, SHAKED N T. Dual-channel low-coherence interferometry and its application to quantitative phase imaging of fingerprints[J]. *Optics Express*, 2012, **20**(24): 26906-26912.

[12] BLAIS F, RIOUX M, BERALDIN J A. Practical considerations for a design of a high precision 3-D laser scanner system[C]. International Society for Optics and Photonics , 1988: 225-246.

[13] BRADLEY B D, CHAN A D C, HAYES M J D. A simple, low cost, 3D scanning system using the laser light-sectioning method[C]. 2008 IEEE Instrumentation and Measurement Technology Conference, 2008, **1**(5): 299-304.

[14] STOCKMAN G C, CHEN S W, HU G, *et al*. Sensing and recognition of rigid objects using structured light[J]. *IEEE Control Systems Magazine*, 1988, **8**(3): 14-22.

[15] HU G Z, STOCKMAN G. 3-D surface solution using structured light and constraint propagation [J]. *IEEE Transactions on Pattern Analysis and Machine Intelligence*, 1989, **11**(4): 390-402.

[16] WANG Yong-chang, LAU D L, HASSEBROOK L G. Fit-sphere unwrapping and performance analysis of 3D fingerprints[J]. *Applied Optics*, 2010, **49**(4): 592-600.

[17] LIU Feng, ZHANG David. 3D fingerprint reconstruction system using feature correspondences and prior estimated finger model[J]. *Pattern Recognition*, 2014, **47**(1): 178-193.

[18] PARZIALE G, DIAZ-SANTANA E, HAUKE R. The surround imager TM: A multi-camera touchless device to acquire 3D rolled-equivalent fingerprints[M]. *Advances in Biometrics*, 2005: 244-250.

[19] FURUKAWA R, SAGAWA R, DELAUNOY A, *et al*. Multiview projectors cameras system for 3D reconstruction of dynamic scenes[C]. IEEE ICCV, 2011: 1602-1609.

[20] BOUGUET J Y. Camera calibration toolbox for Matlab, retrieved http://www. vision. caltech. edu/bouguetj/calib _ doc/.

[21] ZHANG Z Y. A flexible new technique for camera calibration [J]. *IEEE Transactions on Pattern Analysis and Machine Intelligence*, 2000, **22**(11): 1330-1334.

[22] HIRSCHMULLER H, SCHMID C, SOATTO S, *et al*. Accurate and efficient stereo processing by semi-global matching and mutual information [C]. IEEE Computer Society Conference on Computer Vision and Pattern Recognition, 2005, 2: 807-814.